Universitat de Girona
Facultat de Ciències

Resonance-Assisted Hydrogen Bonding controlling excited state Proton Transfer

Student: Nil Prieto Velasco

nilprieto1000@gmail.com

Grau en Química

Tutor: Sílvia Simon Rabasseda

silvia.simon@udg.edu

Institut de Química Computacional i Catàlisi

June 6, 2023

CONTENTS

Resum

Els Enllaços d'Hidrogen Assistits per Ressonància (RAHB, per les seves sigles en anglès) són sistemes en què un enllaç d'hidrogen i un sistema heteroconjugat (constituït per un grup donador de protons i un grup acceptor de protons) formen una estructura cíclica coneguda com un *quasi*-anell. Aquests sistemes presenten un enllaç significativament més fort en comparació amb els enllaços d'hidrogen convencionals a causa dels efectes de ressonància induïts pels electrons π. En aquest estudi s'han investigat sistemes RAHB amb diferents grups donadors de protons (PD) i acceptors de protons (PA) basats en oxigen i nitrogen. Els grups PD inclouen OH i NH2, mentre que els grups PA consisteixen en CHO i CHNH. També, s'han anat diferents anells de 6 membres (6-MRs) en diferents conformacions, donant com a resultat cinc topologies diferents: benzè, lineal, ziga-zaga, L4 i K4.

L'objectiu principal d'aquest estudi és examinar els factors que influeixen en la fortalesa dels RAHB i en la transferència de protons en estats singlet i triplet. Més concretament, s'estudia la influència dels substituents PD i PA en la posició orto d'un 6-MR dins les diferents topologies esmentades anteriorment. L'anàlisi ha implicat 20 sistemes RAHB diferents, utilitzant el nivell de teoria B3LYP/6-311+G(d,p).

S'han recopilat les distàncies dels enllaços d'hidrogen, juntament amb les energies d'activació associades al procés de transferència intramolecular de protons en estat excitat (ESIPT, per les seves sigles en anglès) en els estats de singlet i triplet.

Un altre aspecte important d'aquest estudi és l'anàlisi de la relació entre l'aromaticitat i la fortalesa dels enllaços d'hidrogen. Per a fer-ho, s'han utilitzat índexs d'aromaticitat, més concretament l'índex de para-deslocalització (PDI), que serveix per quantificar la deslocalització dels electrons dins de l'anell. S'ha donat especial atenció a l'anell *ipso,* ja que és un factor determinant en la fortalesa dels RAHB.

En examinar els diversos aspectes dels sistemes RAHB, incloent les energies d'activació, les distàncies dels enllaços d'hidrogen i els índexs d'aromaticitat, aquest estudi pretén proporcionar coneixements valuosos sobre el comportament i les propietats d'aquests sistemes, per millorar la nostra comprensió de la formació d'enllaços d'hidrogen assistits per resonància i el seu impacte en els mecanismes de transferència de protons.

Resumen

Los Enlaces de Hidrógeno Asistidos por Resonancia (RAHB, por sus siglas en inglés) son sistemas en los cuales un enlace de hidrógeno y un sistema heteroconjugado (un grupo donador de protones y un grupo aceptor de protones) forman una estructura cíclica conocida como un *cuasi*-anillo. Estos sistemas presentan un enlace significativamente más fuerte en comparación con los enlaces de hidrógeno convencionales debido a los efectos de resonancia inducidos por los electrones π.

Este estudio investiga sistemas RAHB con diferentes grupos donadores de protones (PD) y aceptores de protones (PA) basados en el oxígeno y nitrógeno. Los grupos PD incluyen OH y NH2, mientras que los grupos PA consisten en CHO y CHNH. También, se van añadiendo diferentes anillos de 6 miembros (6-MRs), lo que resulta en cinco topologías distintas: benceno, lineal, en zigzag, L4 y K4.

El objetivo principal de este estudio es examinar los factores que influyen en la fortaleza de los RAHB y en la transferencia de protones en estados singlete y triplete. Mas concretamente, se estudia la influencia de los sustituyentes PD y PA en la posición orto de un 6-MR dentro de las diferentes topologías. El análisis ha involucrado 20 sistemas RAHB diferentes, utilizando el nivel de teoría B3LYP/6-311+G(d,p).

Se han recopilado las distancias de los enlaces de hidrógeno, junto con las energías de activación asociadas al proceso de transferencia intramolecular de protones en estado excitado (ESIPT, por sus siglas en inglés) en sus estados de singlete y triplete.

Otro aspecto importante de este estudio es el análisis de la relación entre la aromaticidad y la fortaleza de los enlaces de hidrógeno. Para hacer esto, se han utilizado índices de aromaticidad, más concretamente el índice de paradelocalización (PDI), que sirve para cuantificar la deslocalización de los electrones dentro del anillo. Se ha dado especial atención al anillo *ipso* ya que es un factor determinante en la fortaleza de RAHB.

Al examinar los diversos aspectos de los sistemas RAHB, incluyendo las energías de activación, las distancias de los enlaces de hidrógeno y los índices de aromaticidad, este estudio pretende proporcionar conocimientos valiosos sobre el comportamiento y las propiedades de estos sistemas, para mejorar nuestra comprensión de la formación de enlaces de hidrógeno asistidos por resonancia y su impacto en los mecanismos de transferencia de protones.

Abstract

Resonance-Assisted Hydrogen Bonds (RAHB) are systems in which a hydrogen bond and a heteroconjugated system (a proton-donor group and a proton-acceptor group) form a cyclic structure known as a *quasi*-ring. These systems exhibit a significantly stronger bond compared to conventional hydrogen bonds due to resonance effects facilitated by π-electrons.

This study investigates RAHB systems with different proton-donor (PD) and proton-acceptor (PA) groups based on oxygen and nitrogen elements. The PD groups include OH and NH2, while the PA groups consist of CHO and CHNH. The systems are further characterized by the addition of different 6-Membered rings (6-MRs), resulting in five distinct topologies: benzene, linear, kinked, L4, and K4.

The primary focus of this study is to examine the factors that influence RAHB strength and proton transfer in both singlet and triplet states. Specifically, the influence of PD and PA substituents in the ortho position of a 6-MR within the different topologies is elucidated. The analysis involved 20 different RAHB systems, using the B3LYP/6-311+G(d,p) level of theory.

Hydrogen bond distances were collected, along with the activation energies associated with the excited-state intramolecular proton transfer (ESIPT) in both singlet and triplet states.

Another significant aspect of this study is to analyze the interplay between aromaticity and HB strength. Aromaticity indices, particularly the para-delocalization index (PDI), are used to quantify electron delocalization within the ring. Emphasis is placed on the *ipso*-ring as it has shown to be a determining factor in RAHB strength.

By examining the various aspects of RAHB systems, including activation energies, hydrogen bond distances, and aromaticity indices, this study aims to provide valuable insights into the behavior and properties of these systems, enhancing our understanding of resonance-assisted hydrogen bonding and its impact on proton transfer mechanisms.

Ethics Reflection:

In the field of computational chemistry, ethical considerations are a key role to research and it's applications. One ethical concern is responsibly using available data sources while guaranteeing confidentiality through protocols, and using the data only for its intended goal.

Another ethical consideration is the potential to misusing of computational techniques. It is important for researchers to exercise caution and ethical judgment when their work has implications in fields such as pharmaceutical development, environmental impact assessments, or even military applications.

Computational chemist's researchers should prioritize transparency and reproducibility. By making their investigation methods, scripts used and data found openly accessible, because it would ensure the fiability and validity of the results.

Gender Reflection:

In computational chemistry, it is crucial to reflect on gender representation and equality within the field. Historically, science has been dominated by male researchers, leading to gender disparities in research opportunities, funding, and recognition. Efforts must be made to address these disparities and create a more inclusive environment for all genders.

Increasing gender diversity in computational chemistry not only promotes fairness but also improves the quality of research. Diverse perspectives and experiences contribute to innovative problem-solving. Encouraging and supporting women's participation in computational chemistry through mentorship programs, scholarships, and inclusive hiring practices can help promote equal opportunities.

Sustainability Reflection:

In the context of computational chemistry, sustainability considerations are vital to ensure responsible and environmentally conscious research. Energy consumption is a significant concern in computational chemistry due to the high computational power required for simulations and modeling. Researchers should try to optimize algorithms, software, and hardware to minimize energy usage and improve computational efficiency.

Computational chemistry can aid in the understanding of environmental phenomena, such as climate change or pollution. Models and simulations can provide insights into the behavior of

pollutants, the impact of chemicals on ecosystems, or the efficiency of renewable energy technologies. By leveraging computational chemistry in these areas, researchers can contribute to the development of sustainable solutions.

1. Introduction

Hydrogen bonds (HB) play a crucial role in various chemical and biological processes. As Grosch *et al. [1]* described, HB are a type of intermolecular force that arises from the attraction between a hydrogen atom covalently bonded to an electronegative atom (donor) and another electronegative atom (acceptor) in a neighboring molecule. This interaction creates a relatively strong dipole-dipole attraction between the two molecules.

The significance of hydrogen bonds can be seen in their involvement in numerous biological phenomena. For example, in DNA, hydrogen bonds between complementary base pairs contribute to the stability and double-helix structure of the molecule.

Hydrogen bonds also have a profound impact on the physical properties of substances. A notable example is water, where hydrogen bonding between water molecules gives rise to its unique properties, which are crucial for the existence of life as we know it and have far-reaching implications in fields such as biology, chemistry, and environmental science.

Understanding the nature and characteristics of hydrogen bonds allows scientists to design and manipulate molecular structures, develop new materials with specific properties, and design drugs that interact with biological targets through hydrogen bonding interactions.

The introduction of the concept of Resonance-Assisted Hydrogen Bonds (RAHB) by Gilli et al. [2] highlights the importance of studying hydrogen bonding interactions in conjugated systems. RAHBs involve the interaction between a hydrogen bond donor and acceptor that are both part of a conjugated system, allowing for stronger hydrogen bonds compared to conventional ones.

One example of a molecule that exhibits intramolecular proton transfer and demonstrates the presence of RAHB is malonaldehyde. The resonance structures shown in Figure 1a illustrate the delocalization of π electrons within the *quasi*-ring, which contributes to the increased strength of the hydrogen bond. This resonance energy arising from the conjugated system enhances the stability of the RAHB and makes it stronger than conventional hydrogen bonds.

Another significant system where RAHB plays a crucial role is o-hydroxybenzaldehyde (Figure 1b). Similar to malonaldehyde, it benefits from the delocalization of π electrons within the *quasi*-ring, leading to additional stabilization. However, in this case, the C=C π electrons are shared

with the benzene ring, reducing their availability for strengthening the RAHB system. This distinction highlights the influence of the molecular structure on the strength and characteristics of RAHBs.

The study of RAHBs in conjugated systems provides valuable insights into the interplay between hydrogen bonding and aromaticity, allowing for the design and modulation of stronger hydrogen bonds. Understanding the factors that govern the strength and stability of RAHBs contributes to the development of new functional materials and catalysts.

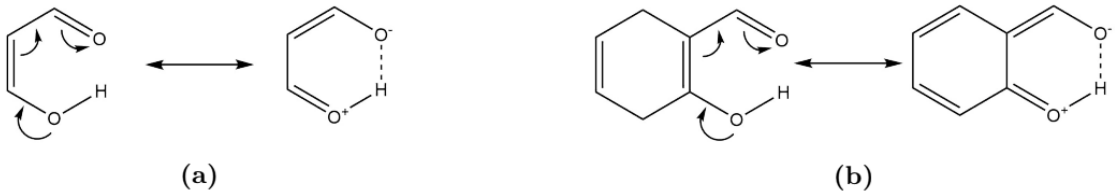

Figure 1: Resonance structures for (a) malonaldehyde and (b) o-hydroxybenzaldehyde taken from reference [3].

Recent studies have shown that RAHB enhancement or weakening can be controlled by not only with the addition of different six-membered rings (6-MRs) but also with the topology and by changing the substituents that present these rings. Pareras *et al*. [3] found that in 1,3-dihydroxyaryl-2-aldehydes the position of the *quasi*-ring formed by the substituents interacting through RAHB influences the strength of the H-bonding, the HBs being stronger when a kinked-like structure is generated by formation of the *quasi*-ring rather than in linear-like structures.

This can be explained using Clar's π-sextet model, which states the Kekulé resonance structure with the largest number of disjoint aromatic π-sextets is the most important.

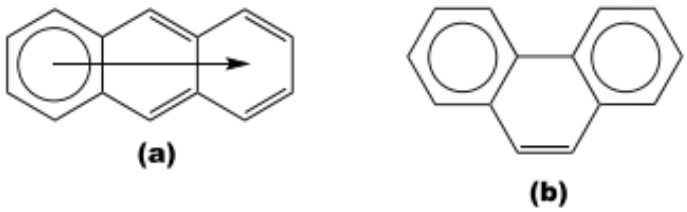

Figure 2: Clar structures for (a) Anthracene and (b) Phenantrene taken from reference [3].

Following this rule, the Clar's structures for [3]acene (anthracene) and [3]phenacene

(phenanthrene) are the ones represented in Figure 2 . [n]Acenes (linear-like structure) with a migrating π-sextet have similar aromaticity in all rings, whereas in [n]phenacenes (kinked-like structure) the outer rings are more aromatic than the central one. Moreover, [n]phenacenes have a larger number of aromatic π-sextets than the corresponding [n]acenes and therefore are more stable and more aromatic as a result of more stabilizing π interactions .

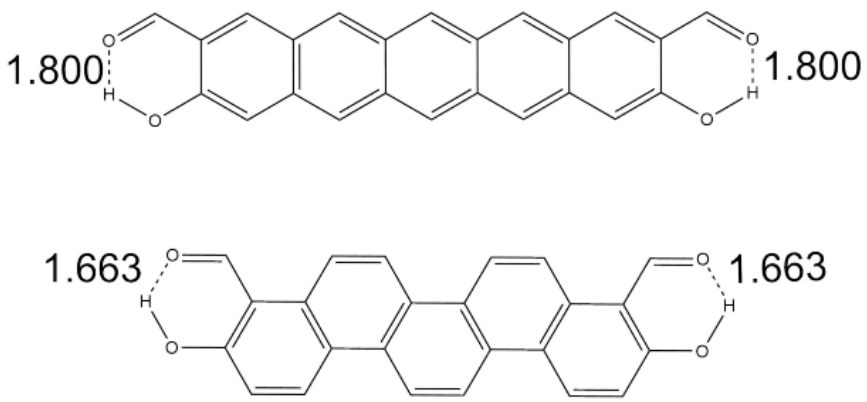

Figure 3: Linear and kinked structures taken from reference [3]. Distances in Å.

Figure 3 shows the difference in the HB length when the different 6-MRs are added within a kinked topology (with a length of 1.663 Å) which presents a stronger HB than the linear chain (with a length of 1.800 Å). As can be seen, the addition and position of the rings can alter the strength of the intramolecular HB.

The increase of strength of the HB can help the tautomerization of these compounds. This structural change is important mainly in the excited state, not only in the singlet one (S_1) but also in the triplet one (T1), and can help to change the photophysics of different molecules. In 2002 , Gilli *et al.* [4] found that in ketohydrazone (Figure 2V) , the weak N-H...O bond can be switched to a stronger O-H...N bond by condensation with a phenyl ring (Figure 2VI) , which greatly stabilizes the O-H...N form stabilizing the different resonance structures.

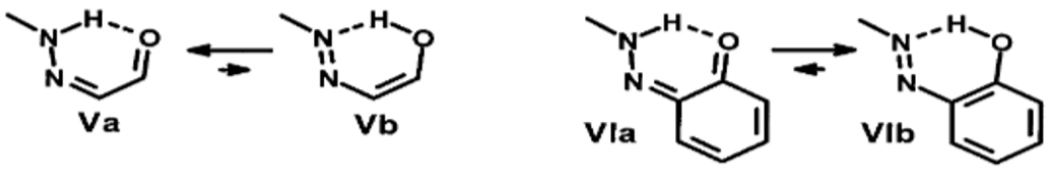

Figure 4: Resonance structures in ketohydrazone series taken from reference [4]

Recently, it was found that not only the topology of different compounds can help tune the HB strength in the ground state, but also the behavior in the triplet state. So, an Excited-State Intermolecular Proton Transfer (ESIPT) can be found, in which the excitation of the molecule to a higher energy state (either S1 or T1) can lead to a proton transfer from a proton-donor group (PD) to a proton-acceptor group (PA), producing a tautomerization of the molecule.

In the electronic ground state, typical ESIPT molecules [5] exist exclusively as an enol (E) form, which is better stabilized by intramolecular H-bond. Upon photoexcitation, however, the redistribution of electronic charge occurs, causing an increase in the acidity of the proton donor and the basicity of the proton acceptor. As a result, fast proton transfer reaction from the proton donor to the proton acceptor takes place along the excited-state potential energy surface via the intramolecular H-bond, leading to a tautomeric transformation from the excited enol form (E*) to the excited keto form (K*) in sub-picosecond time scale. After decaying radiatively to the ground state, reverse proton transfer occurs to their initial E form. This process is shown in figure 5 below.

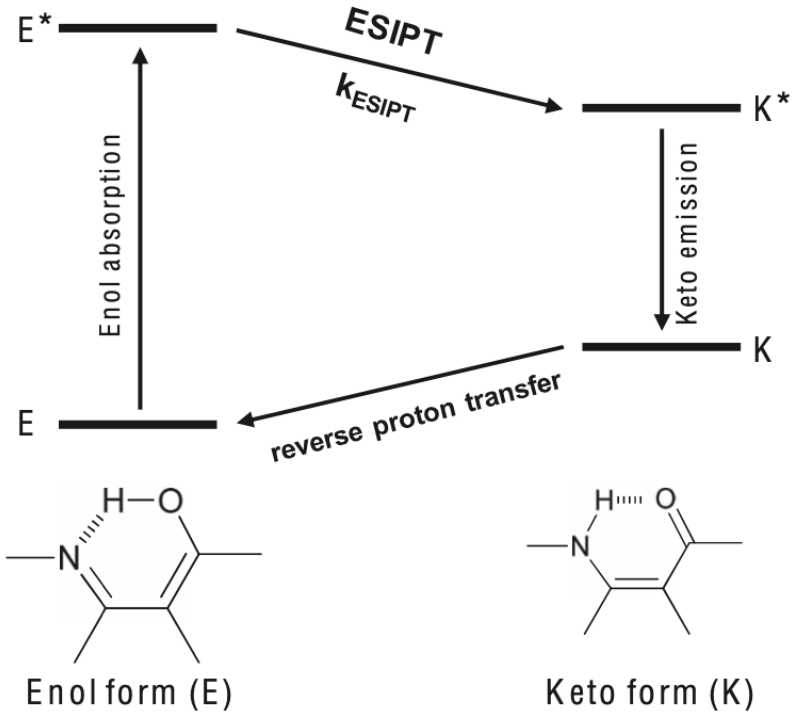

Figure 5: Schematic representation of ESIPT photocycle taken from reference [5]

Kasha, Heldt and Gromin, summarized [6] three cases of ESIPT, each resulting in different spectroscopic phenomena, described by the stability of the ground state (S_0), the singlet excited state (S_1) and the triplet excited state (T_1) of both the normal form and the tautomeric form (which

would correspond to the molecule that has already produced an ESIPT). The cases are represented in figure 6 below.

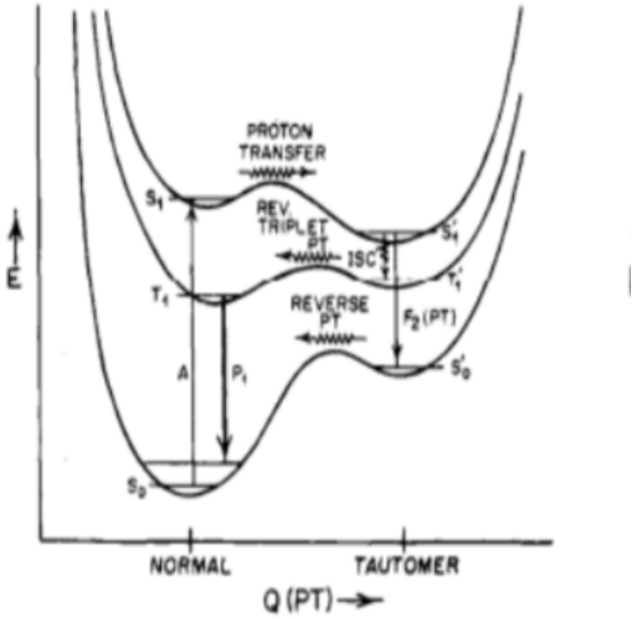

(a)

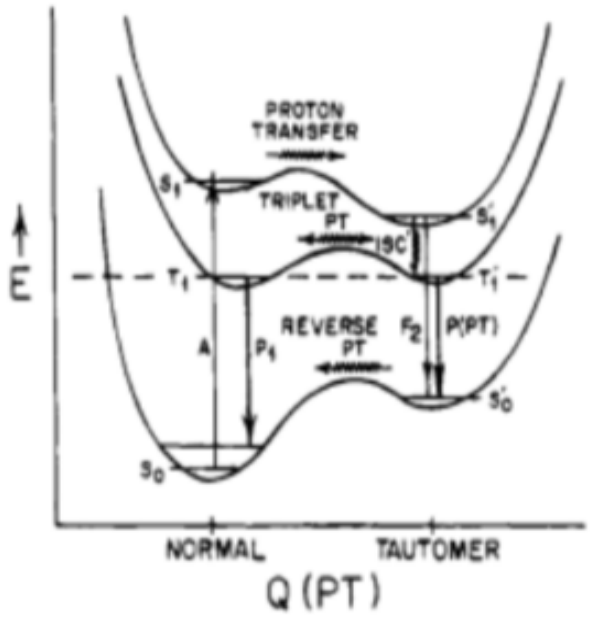

(b)

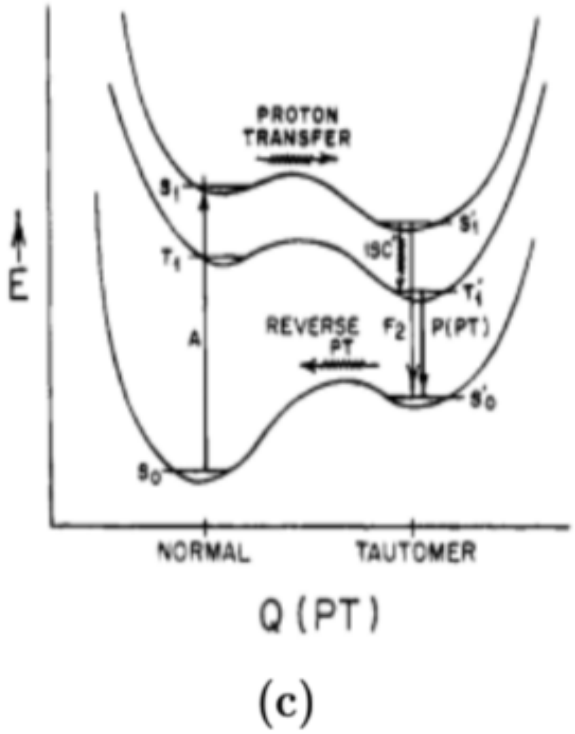

Figure 6: Schematic proton-transfer potentials taken from reference [6]

The three cases differ, as commented before, in the stability of the different states with respect to their respective tautomeric form.

$$(S_0 < S'_0) < (T'_1 < T_1) < (S'_1 < S_1) \qquad (a)$$

$$(S_0 < S'_0) < (T_1 < T'_1) < (S'_1 < S_1) \qquad (b)$$

$$(S_0 < S'_0) < (T'_1 \approx T_1) < (S'_1 < S_1) \qquad (c)$$

In figure 6, we can see different intensity of spectroscopic emissions depending stability of both conformers (normal/ tautomer) of the triplet state.

- Case A. Enhancement of T_1 —> S_0 Phosphorescence via ESIPT: It's assumed that the energy difference T'_1 — T_1 is too great for significant Boltzmann excitation of the T'_1 state from T_1 to occur, even at 298K, so the normal form is the most stable and

phosphorescence (P1 in the figure) is the predominant emission.

- Case B. Dual Phosphorescence (T_1 —> S_0 and T'_1 —> S'_0) via ESIPT: In this case both conformers are approximately isoenergetic so two phosphorescence emissions P1 and P(PT) will compete.

- Case C. Intersystem Crossing after ESIPT with Unique T'_i — S'_0 Phosphorescence : Here, the tautomer is the most stable conformer and only P(PT) is observed.

2. Objectives

The aim of this TFG is to analyze the factors influencing RAHB strength and proton transfer in singlet and triplet state as well as the role of aromaticity in these processes. This objectives can be split in:

- Analyze the modulation of RAHB (resonance-assisted hydrogen bonding) strength in singlet and triplet states, including ground, transition, and first excited states.

- Investigate the activation energies involved in the excited-state intramolecular proton transfer (ESIPT) process, specifically from the ground state to the first excited state, in both singlet and triplet states (S0→S1) and (T0→T1).

- Explore the impact of the presence of both proton acceptor (PA) and proton donor (PD) substituents in the ortho position of different 6-membered rings (6-MRs) on the formation of a quasi-ring. Evaluating how the strength of RAHB changes when the system transitions from the ground state (R) to its first excited state (P), while collecting HB distances.

- Investigate the relationship between changes in the aromaticity of the *ipso*-ring and proton transfer when transitioning from singlet to triplet states. Utilize the para-delocalization index (PDI) as an indicator of aromaticity.

3. Methodology

All calculations were performed using Gaussian 16 [7]. The density functional theory (DFT) method B3LYP [8] was employed, using 6-311+G(d,p) as basis set [9] . Diffusion functions were added, indicated by the "+" sign, and two polarization functions (** or (d,p)) were included. The choice of this basis set was based on previous theoretical studies [10, 11]. Visualization and data extraction were carried out using Chemcraft [12].

All structures were optimized to obtain minima on the potential energy surface (PES) with positive frequencies in reactants and products, and imaginary frequencies in transition states.

Five distinct topologies containing different number of 6-membered rings (6-MRs) have been chosen for analysis: benzene, linear, kinked, l4, and k4. These topologies contained 1 PD (proton donor) and 1 PA (proton acceptor) group based on Oxygen and Nitrogen. The PA groups examined were CHO and CHNH, while the PD groups were OH and NH2, resulting in 20 combinations of PD, PA, and different topologies.

Upon optimization, not all systems exhibited resonance-assisted hydrogen bonding (RAHB) due to several impediments. For each system, three different conformers were analyzed: the reactants (enolic form), transition state (TS), and products (keto form). The free energy differences ($\Delta G_{R\rightarrow TS}$ and $\Delta G_{R\rightarrow P}$) were taken into account along with the hydrogen bond (HB) distances, as indicators of RAHB strength.

In order to calculate the aromaticity, the ESI-3D program [13, 14, 15] was employed. The para-delocalization index (PDI) was used as an electronic-based descriptor of aromaticity.

To explicate the behaviors of certain triplet molecules, the spin density was depicted, representing the difference between the alpha and beta electron densities and accounting for the presence of unpaired electrons. The graphical representation of spin density was generated using Chemcraft [12] with a contour of 0.005 atomic units (ua).

4. Results and Discussion

This work is an extension of Grèbol [10] and Samaniego [11] TFG works. The primary focus of this research is to investigate resonance-assisted hydrogen bond (RAHB) systems involving various proton donor (PD) and acceptor (PA) groups.

Specifically, the investigation will study how different substituted 6-MRs behave in both singlet and triplet ground state and first excited state embracing the characterization of ground state (S_0 , T_0), transition state (TS) and first excited state (S_1 , T_1), as well as the role of aromaticity in this process.

To facilitate a comprehensive analysis, five distinct topologies have been chosen for analysis: benzene (B), linear (L), kinked (K), L4, and K4, as reproduced in Figure 7. Each topology incorporates a proton acceptor group (X) and a proton donor group (YH) in orto position to each other, interacting with a HB, so forming a *quasi*-ring. By examining these diverse configurations, a comprehensive understanding of RAHB systems can be achieved.

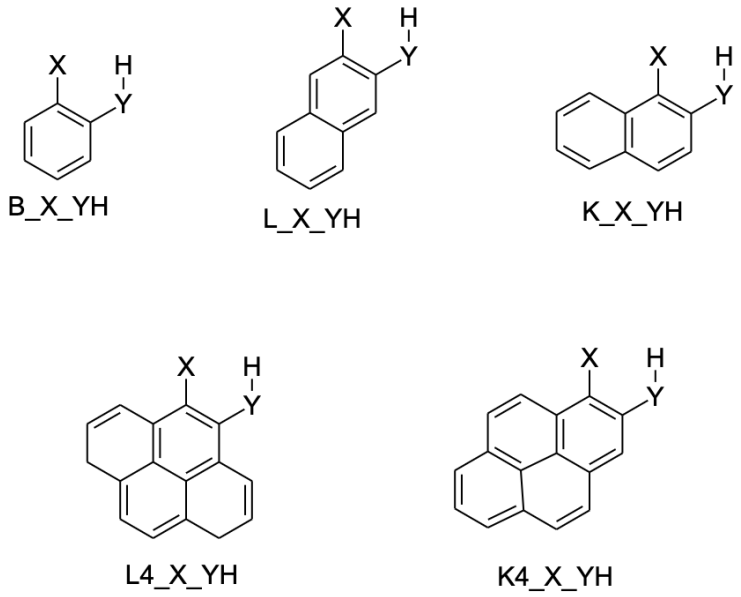

Figure 7: Schematic representation of different topologies.

4.1 Proton transfer

The initial phase of the present study will involve an examination of the activation energies associated with the proton transfer process, specifically the excited-state intramolecular proton

transfer (ESIPT), from the ground state to the first excited state in both singlet and triplet states; ($S_0 \rightarrow S_1$) and ($T_0 \rightarrow T_1$).

As it was explained in the introduction, the strength of RAHB is related to the proton transfer process. As mentioned before, Kasha *et al.* [6] described 3 possible cases where the normal and tautomeric forms coexist (Figure 6), but in some cases only one conformer is stable (Figures 8A' and 8C') .

In figure 8, we can see 5 different scenarios for the proton-transfer potential wells, the normal form corresponding to the reactant (enol form) and the tautomer corresponding to the PT product (keto form) as represented in reference [6]. The qualitative data of the results demonstrated in this project is shown in Table 1.

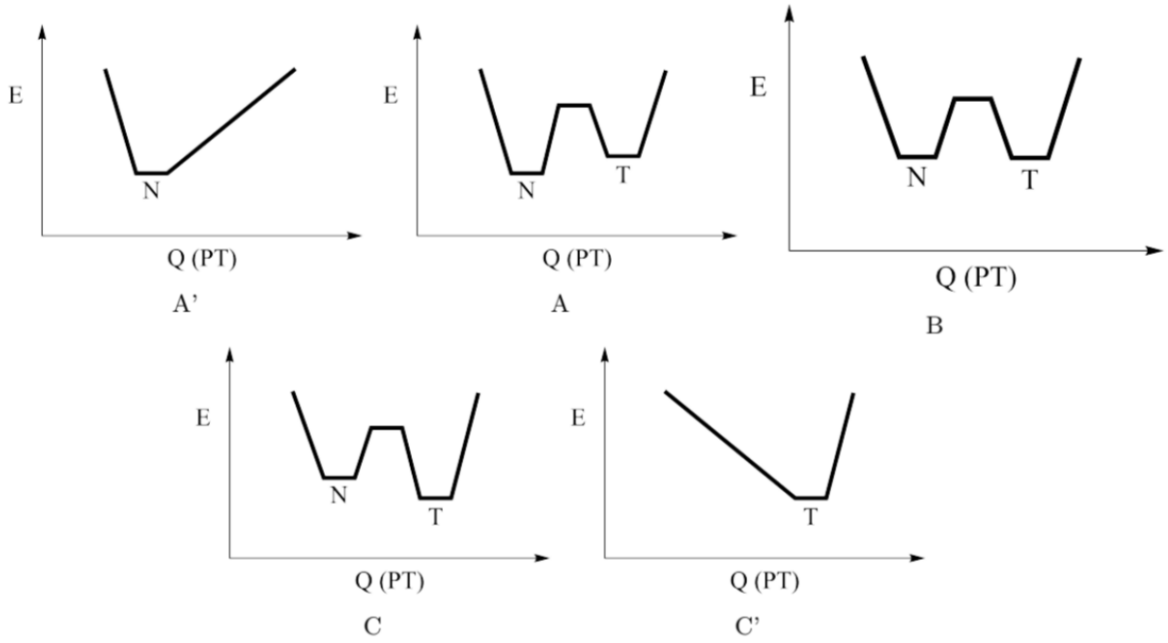

Figure 8: Different scenarios depending on the stability of different tautomers taken from [7]

Table 1 has been structured to present the information by arranging the columns according to different topologies, while the rows correspond to various combinations of substituent groups (the first letter representing the proton-acceptor group, followed by the proton-donor group). Each topology is further divided into three additional columns: the first column denotes the free energy difference between the reactant and the transition state ($\Delta G_{R \rightarrow TS}$), the second column represents the free energy difference between the reactant and the product ($\Delta G_{R \rightarrow P}$), and the third column provides a qualitative classification based on the five cases reproduced in Figure 8.

A qualitative classification was made according to the following criteria:

- Case A' : Only reactant (enolic form) is formed.
- Case A : $\Delta G_{R\rightarrow P}$ > 2 kcal/mol (reactant more stable).
- Case B : 2 kcal/mol > $\Delta G_{R\rightarrow P}$ > -2 kcal/mol
- Case C : $\Delta G_{R\rightarrow P}$ < -2 kcal/mol (product more stable).
- Case C' : Only product (keto form) is formed.

The nomenclature employed in this study follows the format ARO_XYH_M, where ARO represents the topology (B, L, K, L4, K4), X denotes the proton-acceptor group (O for CHO, N for CHNH), YH signifies the proton-donor group (O for OH, N for NH_2), and M indicates the multiplicity (S for singlet, T for triplet).

For instance, the designation B_ON_T refers to a benzene molecule in its triplet state, with CHO as the proton-acceptor group and NH_2 as the proton-donor group. This molecule exhibits a free energy difference of $\Delta G_{R\rightarrow TS}$ = 0.60 kcal/mol and $\Delta G_{R\rightarrow P}$ = -2.97 kcal/mol, as detailed in Table 1.

In some instances, the complete name is not explicitly stated, as the omitted part applies to all molecules. For example, when mentioning B_OH, it covers both the triplet and singlet states of the benzene topology with OH as the proton-acceptor group.

Table 1: $\Delta G_{R\rightarrow TS}$ (kcal/mol), $\Delta G_{R\rightarrow P}$ (kcal/mol) and group classification (*) for both singlet and triplet states

		B			L			K			L4			K4		
		ΔG R→TS	ΔG R→P	*	ΔG R→TS	ΔG R→P	*	ΔG R→TS	ΔG R→P	*	ΔG R→TS	ΔG R→P	*	ΔG R→TS	ΔG R→P	*
OO	**S**	-	-	A'	-	-	A'	4,74	4,26	A	2,10	3,31	A	-	-	A'
	T	-	-	C'	-0,60	-6,21	C	1,55	0,48	B	4,59	4,91	A	1,32	0,53	B
ON	**S**	-	-	A'	-	-	A'	-	-	A'	-	-	A'	-	-	A'
	T	0,60	-2,97	C	1,84	-0,10	B	5,25	5,08	A	12,91	14,07	A	5,39	5,13	A
NO	**S**	3,56	3,27	A	6,33	7,46	A	1,00	-1,11	B	-0,15	-4,13	C	2,55	2,44	A
	T	-	-	A'	-	-	C'	-0,35	-6,28	C	2,29	-1,50	B	0,42	-5,44	C
NN	**S**	12,49	13,11	A	15,45	16,53	A	8,31	7,54	A	5,78	5,31	A	11,83	12,54	A
	T	0,75	-10,44	C	1,00	-9,04	C	4,95	-1,23	B	8,73	6,04	A	4,19	-1,63	B

In figure 9, we present the reaction profiles and stability analysis of the NN molecule, which is the only molecule that exhibits both conformers across all its topologies and multiplicities. Upon

examining the NN molecule, we observe that the enolic forms (reactants) consistently represent the most stable form in the singlet state (green lines in Figure 9).

In the case of B_NN_S, the keto form (product) is significantly more unstable (13,11 kcal/mol), and the energy barrier is considerably higher. Upon the addition of a six membered ring (6-MR) in a linear position (L_NN _S), the energy barrier further increases, leading to destabilization of the products. However, when the 6-MR is added in a kinked topology (K_NN _S) the energy barrier decreases, resulting in the stabilization of the products.

By adding two additional 6-MRs, L4_NN _S topology exhibits a lower energy barrier, indicating that the keto form is more stabilized compared to other topologies. On the other hand, the K4_NN _S topology displays an energy profile that closely resembles that of B_NN _S.

In its triplet state (orange line in Figure 9), the products are more stable than their respective singlet isomers in all topologies except for L4_NN _T . Both B_NN _T and L_NN _T exhibit similar energy profiles, with the products being significantly more stable than the reactants (-10,44 kcal/mol and -9,04 kcal/mol, respectively). Similarly, K_NN _T and K4_NN _T also demonstrate similar energy profiles to each other, although the difference between the products and reactants is smaller compared to B_NN _T and L_NN _T. On the contrary, L4_NN _T destabilizes the products more than its singlet isomer.

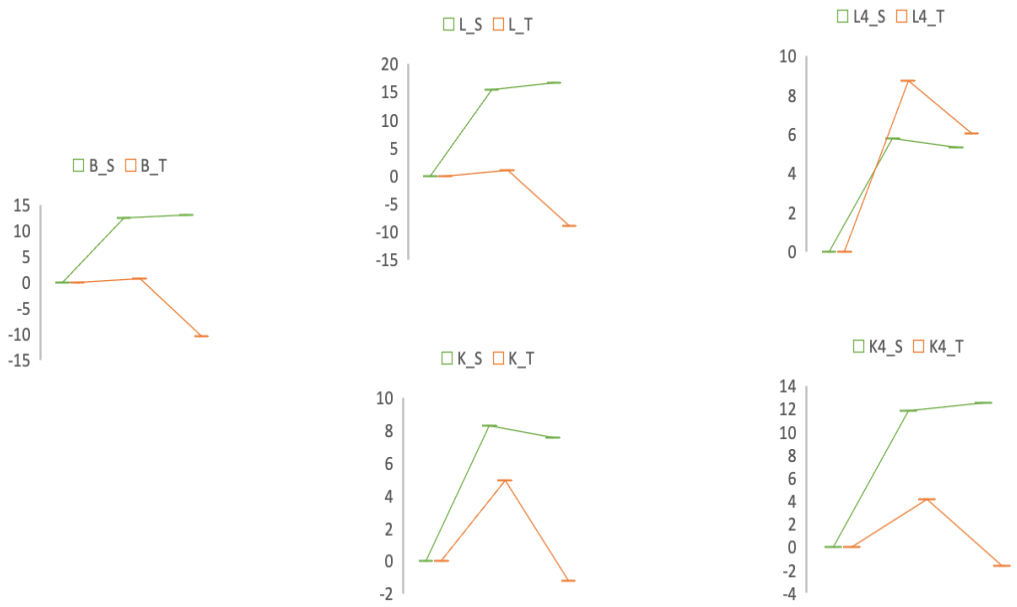

Figure 9: Free energy wells (in kcal/mol) for NN molecule in both single and triplet state.

All these relationships of energy stabilizations discussed so far when adding 6-MRs among different topologies and multiplicities, appear to follow a pattern in all studied molecules, although there are some exceptions.

In general, in all singlets, the products (keto form) are more stable than the reactants (enolic form), and in benzene with triplet multiplicity (B_T), products are more stable than reactants. An unusual case is NO, as K_NO_S and L4_NO_S are the only singlets in where products become more stable than reactants (-1,11 kcal/mol and -4,13 kcal/mol, respectively), whereas in the case of B_NO_T, the only stable form is the reactant, this is different from other B_T cases where the products are more stable than the reactants.

Another noteworthy case is ON, as in its singlet state, it does not exhibit proton transfer (TP) in any case, while in its triplet state, it shows TP in all cases.

Kinked (K) and L4 topologies seem to allow for more TP as they present both conformers in 7 out of 8 cases, while benzene presents the fewest cases with 4 out of 8 cases.

If we take a good look to O and N substituents, we can see that O (CHO) in its singlet state (O_S) only produces proton-transfer in 2 out of 10 molecules while N (CHNH) in its singlet state (N_S) produces PT in 10 out of 10 cases, so O_S is a bad acceptor group compared to N_S.

On the other hand, O (OH) is a better donor group than N (NH_2), because products are more stable when OH behaves as donor rather than when NH_2 does it. i.e: $\Delta G_{R\rightarrow P}$ (K_NN_S) = 7,54 kcal/mol , $\Delta G_{R\rightarrow P}$ (K_NO_S) = -1,11 kcal/mol.

No previous studies were found to compare with the data obtained from this section.

4.2 Hydrogen bond distances

When there is a presence of both PA and PD substituents in orto position in a 6-MR, a *quasi*-ring can be seen. The idea behind this section is to study how will the strength of this RAHB change when the system excited from the ground state (R) its first excited state (P) . The distance of the hydrogen bonds will be collected.

The nomenclature used in this section is the similar to the previous one: ARO_XYH_M_F where ARO= B, L, K, L4, K4 (topology), X= O (CHO), N (CHNH) (proton-acceptor groups), YH= O (OH), N (NH_2) (proton-donor groups), M= S, T (multiplicity) F= R (reactant), P (product).

The arrangement of Table 2 is similar to the one in table 2, but in this case each topology is divided into reactants (enolic form) and products (keto form).

Table 2: HB distances in Å

		B		L		K		L4		K4	
		R	P	R	P	R	P	R	P	R	P
OO	S	1,767	-	1,793	-	1,663	1,398	1,617	1,504	1,681	-
	T	-	1,757	1,475	1,721	1,633	1,642	1,660	1,604	1,631	1,630
ON	S	1,965	-	1,983	-	1,867	-	1,874	-	1,874	-
	T	1,765	1,744	1,796	1,709	1,859	1,660	1,836	1,593	1,836	1,645
NO	S	1,731	1,756	1,751	1,637	1,648	1,774	1,608	1,798	1,665	1,708
	T	1,563	-	-	1,971	1,656	1,886	1,651	1,861	1,638	1,889
NN	S	1,947	1,757	1,957	1,629	1,863	1,771	1,811	1,800	1,871	1,708
	T	1,830	2,008	1,810	1,977	1,909	1,922	1,844	1,898	1,861	1,913

Firstly, we will examine two intriguing cases. The first case involves K4_OO_T, where the HB distance shows a variation of only 0.001 Å during the transition from reactants to products. The second case pertains to B_NO_T, which exhibits a remarkably short HB distance (1.563 Å) but does not produce proton transfer.

Upon revisiting the case of NN and analyzing the hydrogen bond (HB) distances, a consistent trend emerges. When transitioning from the singlet reactant state (S_R) to the singlet product state (S_P), there is a notable decrease in the HB distance. However, an intriguing discrepancy arises when considering the relative stability of NN_P, which exhibits pronounced instability compared to the reactants (NN_R) (as exemplified by L_NN: $\Delta G_{R\rightarrow P}$ = 16.53 kcal/mol). Based on this, one might expect the HB distance in NN_S_R to be smaller than that in NN_S_P. Surprisingly, this expectation is not met.

Shifting our attention to NN_T, the HB distance increases from the reactants to the products. As we have established, the products in NN_T display significantly higher stability compared to the reactants. Consequently, one might anticipate a decrease in the HB bond length, reflecting a stronger interaction. However, the observed increase in the HB distance presents a paradoxical situation again.

Further examination of ON_T reveals a consistent decrease in the HB distance during the transition from the triplet reactant state (T_R) to the triplet product state (T_P) across all considered scenarios, although some topologies stabilize more the products, and other stabilize more the reactants.

Thus, it becomes evident that the changes in HB distances cannot be solely predicted based on the ΔG values derived in the preceding section, as other factors come into play. One such factor that significantly impacts HB interactions is aromaticity, which will be elucidated in the subsequent section, focusing on its role in modulating RAHB systems.

A consistent observation is made when transitioning from the singlet product state (S_P) to the triplet product state (T_P), in where an increase in the HB distance is observed across all cases.

Moreover, it is worth noting that for molecules that exhibit both tautomers within one multiplicity while exclusively presenting the enol form (reactant) within the other multiplicity, a consistent decrease in the HB distance is observed during the transition from S_R to T_R. This can be exemplified by ON, where none of its topologies in the singlet state yield products. Consequently, each transition from S_R to T_R always results in a reduction in the HB distance.

On the other hand, in topologies featuring proton transfer (TP) in both singlet and triplet states, while transitioning from S_R to T_R occasionally results in an increase in the HB distance, as in L4_NO (where S_R = 1.608 Å and T_R = 1.651 Å), there are other cases where the HB distance decreases, such as K4_NO (S_R = 1.665 Å and T_R = 1.638 Å) .

To provide a comprehensive overview of the disparities in HB distances between the singlet and triplet states during the transition from reactants (R) to products (P), Table 3 is presented, illustrating the dynamic nature of HB interactions within the RAHB systems.

Table 3: ΔHB distance (in Å) between singlet and triplet states

	B		L		K		L4		K4	
	R	P	R	P	R	P	R	P	R	P
OO	-	-	0,318	-	0,030	-0,244	-0,043	-0,100	0,050	-
ON	0,200	-	0,187	-	0,008	-	0,038	-	0,038	-
NO	0,168	-	-	-0,334	-0,008	-0,112	-0,043	-0,063	0,027	-0,181
NN	0,117	-0,251	0,147	-0,348	-0,046	-0,151	-0,033	-0,098	0,010	-0,205

When transitioning from singlet to triplet state, the change in HB distances in the products is bigger than the change in reactants. This suggests that the products, are more influenced by the change in multiplicity.

The HB distances in B, L and K topologies are in agreement with previous calculated data by Grèbol [10].

4.3 Aromaticity

In this section, we have examined aromaticity indices, specifically the PDI (paradelocalization index), in order to explain the behavior of the molecules studied in this work. Special attention will be given to the *ipso*-ring as it is a determining factor in the strength of RAHB (resonance-assisted hydrogen bonding).

The PDI provides a measure the delocalization of the electrons within the ring, in singlet state a higher PDI indicates a more aromatic ring. The more aromatic the *ipso*-ring is (PDI2), the more challenging it becomes to engage in RAHB, as the 6 π electrons are more delocalized within the ring and less available for interaction with the *quasi*-ring.

The nomenclature used in this section for the topologies has been written in lowercase instead of uppercase, but it does not imply any change, it means exactly the same thing.

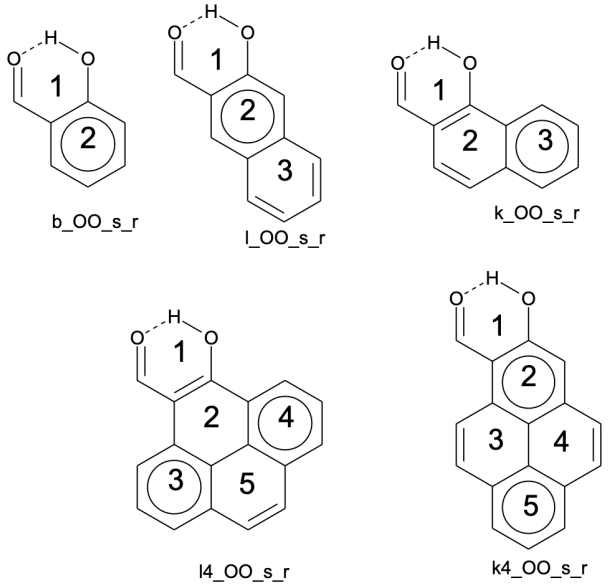

Figure 10: Clark structures for OO_S_R

Figure 10 illustrates Clark structures for OO_S_R. The numbers displayed within the rings correspond to the identifiers used in Table 1. For example, the *quasi*-ring corresponds to PDI1, while the *ipso*-ring corresponds to PDI2. This nomenclature is consistently employed across all XYH cases.

In Table 4, a color system has been employed to facilitate interpretation. Singlets are depicted in bold, reactants are highlighted with an orange background, transition states are shown with a blue background, and products have a white background. This table represents the NN case, the other cases being represented in the appendix.

PDI provides a measure the delocalization of the electrons within the ring. In singlet state a higher PDI indicates a more aromatic ring. The more aromatic the *ipso*-ring is (PDI2), the more challenging it becomes to help to strength RAHB, as the 6 π electrons are more delocalized within the ring and less available for interaction with the *quasi*-ring.

Table 4: PDI Values (in e) for the different rings in NN molecule for reactants, transition state and products

	PDI1	PDI2	PDI3	PDI4	PDI5
b_NN_S_P	**0.042**	**0.057**	-	-	-
b_NN_S_R	**0.024**	**0.079**	-	-	-
b_NN_S_TS	**0.041**	**0.064**	-	-	-
b_NN_T_P	0.011	0.050	-	-	-
b_NN_T_R	0.014	0.039	-	-	-
b_NN_T_TS	0.014	0.041	-	-	-
k_NN_S_P	**0.041**	**0.032**	**0.082**	-	-
k_NN_S_R	**0.029**	**0.053**	**0.077**	-	-
k_NN_S_TS	**0.042**	**0.040**	**0.080**	-	-
k_NN_T_P	0.015	0.041	0.065	-	-
k_NN_T_R	0.014	0.026	0.072	-	-
k_NN_T_TS	0.017	0.030	0.067	-	-
l_NN_S_P	**0.039**	**0.054**	**0.058**	-	-
l_NN_S_R	**0.017**	**0.060**	**0.070**	-	-
l_NN_S_TS	**0.037**	**0.055**	**0.060**	-	-
l_NN_T_P	0.013	0.023	0.067	-	-
l_NN_T_R	0.028	0.024	0.054	-	-
l_NN_T_TS	0.026	0.021	0.059	-	-
k4_NN_S_P	**0.040**	**0.037**	**0.032**	**0.055**	**0.067**
k4_NN_S_R	**0.024**	**0.051**	**0.039**	**0.047**	**0.068**

k4_NN_ S_TS	**0.039**	**0.042**	**0.034**	**0.052**	**0.067**
k4_NN_ T_P	0.016	0.021	0.053	0.042	0.055
k4_NN_ T_R	0.025	0.024	0.055	0.057	0.038
k4_NN_ T_TS	0.030	0.020	0.056	0.048	0.045
l4_NN_ S_P	**0.040**	**0.019**	**0.072**	**0.075**	**0.045**
l4_NN_ S_R	**0.033**	**0.030**	**0.069**	**0.071**	**0.044**
l4_NN_ S_TS	**0.043**	**0.023**	**0.071**	**0.073**	**0.044**
l4_NN_ T_P	0.020	0.026	0.060	0.065	0.046
l4_NN_ T_R	0.011	0.029	0.047	0.044	0.059
l4_NN_ T_TS	0.018	0.023	0.059	0.057	0.050

If we examine the PDI2 (*ipso*-ring) of b_NN_S, a decrease is observed upon going from reactants to products, with corresponding values of 0.079 e and 0.056 e, respectively. This reduction consistently occurs when transitioning from S_R to S_P. The PDI value in the singlet state serves as an indicator of aromaticity, where a larger PDI value signifies a greater aromatic character of the ring. Heightened aromaticity in the *ipso*-ring corresponds to decreased RAHB propensity, resulting in heightened stability of the reactants. Consequently, $\Delta G_{R\rightarrow P}$ remains positive in all cases, as shown in Table 1. This correlation is further substantiated by the HB bond distances, which are comparatively larger in reactants than in products due to the weaker tendency to give RAHB (Table 2).

Considering the *quasi*-ring as a conventional ring, the linear (l) and kinked (k) topologies exhibit resemblance to anthracenes and phenanthrenes in Figure 3, respectively. As previously elucidated [3], in the singlet state, aromaticity across anthracenes remains constant across all rings, while in phenanthrenes, the outer rings are more aromatic than the inner rings. Analyzing the PDI values of ring 2 (*ipso*-ring) and ring 3 (the ring furthest from the *quasi*-ring) in l_NN_S_P, the values are similar; PDI2 = 0.054 e and PDI3 = 0.058 e, thus indicating similar aromaticities. Conversely, in k_NN_S_P; PDI2 = 0.032 e and PDI3 = 0.082 e (denoting different aromaticities). The same pattern is mirrored within the reactants.

The PDI of the *ipso*-ring enables an estimation of RAHB strength, thus any variations in this value will impact RAHB strength.

In l_NN_S_R, PDI2= 0.059 e, yet upon excitation to the triplet state, it experiences a significant alteration (0.024 e). This alteration results in a distinct behavior in the molecule between singlet and triplet states, as depicted in Figure 9. Conversely, in l4_NN, PDI2 exhibits a small variation,

thereby producing minimal changes in stability across various multiplicities.

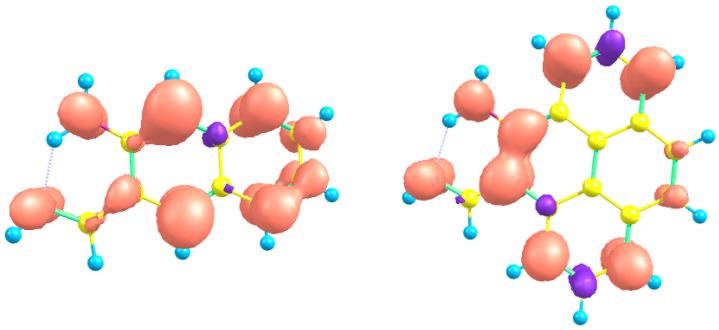

Figure 11: SCF density for l_NN_T_R and l4_NN_T_R respectivetly.

To explicate this different behavior, Figure 11 illustrates the spin densities (SCF) of l_NN_T_R and l4_NN_T_R. These spin densities provides information of where are electron unpaired when going from S to T. The *ipso*-ring of l4 remains unaffected by this transition, as the spin density primarily resides in rings 3 and 4. Conversely, in the linear case, the *ipso*-ring exhibits substantial spin density, indicating the occurrence of unpaired electrons during the transition from singlet to triplet states, thereby occasioning different behavior.

PDI values for OO are consistent with the ones obtained in. [3, 16].

As has been observed, the behavior is quite similar when the electrons are not unpaired in the *ipso*-ring. However, when the unpaired electrons are present in the *ipso*-ring, the proton transfer in the triplet state is clearly affected due to the role played by the aromaticity of the *ipso*-ring.

The presence of unpaired electrons in the *ipso*-ring introduces significant changes in the properties and reactivity of the system. The aromaticity of the *ipso*-ring plays a crucial role in the stability and proton transfer capability. It influences the electron delocalization and distribution within the ring, which in turn affects the energy barriers and electronic states involved in the proton transfer process. The aromaticity of the *ipso*-ring can modulate the interactions between the proton donor and acceptor, leading to variations in the strength and efficiency of the proton transfer mechanism.

5. Conclusions

Based on the analysis of 20 different RAHB systems with various topologies at the B3LYP/6-311+G(d,p) level of theory, the following conclusions can be organized for better comprehension and cohesion:

- The presence of 6-membered rings (6-MRs), and different proton acceptor (PA) and proton donor (PD) groups have been demonstrated to significantly influence the strength of RAHB.

- O (OH) is a more effective donor group compared to N (NH2), as evidenced by the increased stability of products when OH acts as the donor. Among all the PD and PD combinations, only NN exhibits both conformers in both multiplicities and across all topologies.

- The inclusion of 6-MRs in RAHB systems, mostly in kinked (K) and L4 topologies, facilitates proton transfer more effectively than benzene (B).

- Examining the stability of enolic (reactant) and keto (product) forms in singlet and triplet states reveals that the reactant is the most stable form in the singlet state. Transitioning from singlet to triplet state in the keto form leads to an increase in the hydrogen bond (HB) distance across all studied cases. However, in the enolic form, when one multiplicity stabilizes only one conformer, the transition from singlet to triplet state results in a decrease in the HB distance.

- The change in HB distances in the reactants is smaller compared to the products when transitioning from singlet to triplet state, indicating a stronger influence of multiplicity on the keto form.

- The aromaticity of the *ipso*-ring plays a crucial role in modulating the interactions between the proton donor and acceptor, thereby influencing the strength and efficiency of the proton transfer mechanism. L4 topology exhibited a small variation in the aromaticity of the *ipso*-ring, whereas B and L topologies exhibited significant changes.

References

[1] Grosch, A. A., Van Der Lubbe, S. C. C., & Fonseca Guerra, C. (2018). Nature of intramolecular resonance assisted hydrogen bonding in malonaldehyde and its saturated analogue. The Journal of Physical Chemistry A, 122(6), 1813-1820.

[2] Gilli, G., Bellucci, F., Ferretti, V., & Bertolasi, V. (1989). Cheminform abstract: Evidence for resonance-assisted hydrogen bonding from crystal-structure correlations on the enol form of the β-diketone fragment. ChemInform, 20(20).

[3] Gerard Pareras et al. (Dec. 2019) “Tuning the Strength of the Resonance-Assisted Hydrogen Bond in Acenes and Phenacenes with Two o -Hydroxyaldehyde Groups—The Importance of Topology”. The Journal of Organic Chemistry 84.23 15538–15548.

[4] Gilli, P et al. (2002). The nature of solid-state N−H···O/O−H···N tautomeric competition in resonant systems. Intramolecular proton transfer in low-barrier hydrogen bonds formed by the ···O=C-C=N-NH···⇄···HO-C=C-N=N··· ketohydrazone−azoenol system. A variable-temperature x-ray crystallographic and dft computational study. Journal of the American Chemical Society, 124(45), 13554-13567.

[5] Kwon, J. E., & Park, S. Y. (2011). Advanced organic optoelectronic materials: Harnessing excited-state intramolecular proton transfer (Esipt) process. Advanced Materials, 23(32), 3615-3642.

[6] Kasha, M., Heldt, J., & Gormin, D. (1995). Triplet state potentials in the competitive excitation mechanisms of intramolecular proton transfer. The Journal of Physical Chemistry, 99(19), 7281-7284.

[7] M. J. Frisch et al. Gaussian˜16 Revision A.03. Gaussian Inc. Wallingford CT. (2016).

[8] Jens Antony and Stefan Grimme. “Density functional theory including dispersion corrections for intermolecular interactions in a large benchmark set of biologically relevant molecules”. en. In: Physical Chemistry Chemical Physics 8.45 (2006), p. 5287.

[9] R. Krishnan et al. “Self-consistent molecular orbital methods. XX. A basis set for correlated wave functions”. en. In: The Journal of Chemical Physics 72.1 (Jan. 1980), pp. 650– 654

[10] Grèbol, J. Simon S. (2022). "Proton donor and acceptor effect on the excitation energy of

Resonance Assisted Hydrogen Bond systems". TFG. Universitat de Girona

[11] Samaniego, M. Simon S. (2021). “Tuning RAHB strength exciting from singlet to triplet state with different topology of PAHs chains”. TFG. Universitat de Girona.

[12] Chemcraft - Graphical program for visualization of quantum chemistry computations. Version 1.8, build 648 . https://www.chemcraftprog.com/

[13] Matito, E. ESI-3D (2006): Electron Sharing Indices Program for 3D Molecular Space Partitioning; Institute of Computational chemistry and Catalysis (IQCC), Universitat de Girona

[14] Matito, E., Duran, M., & Solà, M. (2005). The aromatic fluctuation index (FLU): A new aromaticity index based on electron delocalization. The Journal of Chemical Physics, 122(1), 014109.

[15] Matito, E., Solà, M., Salvador, P., & Duran, M. (2007). Electron sharing indexes at the correlated level. Application to aromaticity calculations. Faraday Discuss., 135, 325–345.

[16] Palusiak, M., Simon, S., & Solà, M. (2006). Interplay between intramolecular resonance-assisted hydrogen bonding and aromaticity in o -hydroxyaryl aldehydes. The Journal of Organic Chemistry, 71(14), 5241-5248.

Appendix

Table 5: PDI Values (in e) for the different rings in OO molecule for reactants, transition state and products.

	PDI1	PDI2	PDI3	PDI4	PDI5
b_OO_s_r	**0.023286**	**0.081448**			
b_OO_t_p	0.010765	0.043763			
k_OO_s_p	**0.039718**	**0.036667**	**0.082424**		
k_OO_s_r	**0.028969**	**0.053922**	**0.077892**		
k_OO_s_ts	**0.039759**	**0.036850**	**0.082366**		
k_OO_t_p	0.013491	0.034643	0.059833		
k_OO_t_r	0.012667	0.026044	0.066677		
k_OO_t_ts	0.015941	0.028762	0.063529		
l_OO_s_r	**0.016771**	**0.061568**	**0.070130**		
l_OO_t_p	0.015073	0.021460	0.065526		
l_OO_t_r	0.027496	0.023791	0.055883		
l_OO_t_ts	0.027139	0.023084	0.057114		
k4_OO_s_r	**0.023196**	**0.052027**	**0.039952**	**0.047928**	**0.068052**
k4_OO_t_p	0.022235	0.018119	0.054600	0.045075	0.049957
k4_OO_t_r	0.024718	0.024633	0.054721	0.057074	0.038506
k4_OO_t_ts	0.031536	0.020022	0.054895	0.051591	0.043080
l4_OO_s_p	**0.039338**	**0.019831**	**0.073378**	**0.475470**	**0.044801**
l4_OO_s_r	**0.032867**	**0.030382**	**0.070958**	**0.466337**	**0.043772**
l4_OO_s_ts	**0.041409**	**0.022907**	**0.072581**	**0.472379**	**0.044481**
l4_OO_t_p	0.015718	0.025392	0.051149	0.470818	0.049128
l4_OO_t_r	0.012897	0.033329	0.046857	0.416288	0.058862
l4_OO_t_ts	0.018264	0.025010	0.054830	0.453728	0.051681

Table 6: PDI Values (in e) for the different rings in ON molecule for reactants, transition state and products.

	PDI1	PDI2	PDI3	PDI4	PDI5
b_ON_s_r	**0.023982**	**0.078103**			
b_ON_t_p	0.011731	0.049427			
b_ON_t_r	0.012379	0.039105			
b_ON_t_ts	0.014191	0.042030			
k_ON_s_r	**0.029381**	**0.051214**	**0.077634**		
k_ON_t_p	0.014865	0.040109	0.063880		
k_ON_t_r	0.012322	0.025693	0.067752		
k_ON_t_ts	0.015988	0.032496	0.064062		
l_OO_s_r	**0.016771**	**0.061568**	**0.070130**		
l_OO_t_p	0.015073	0.021460	0.065526		

l_OO_t_r	0.027496	0.023791	0.055883		
l_OO_t_ts	0.027139	0.023084	0.057114		
k4_ON_s_r	**0.023978**	**0.050394**	**0.038966**	**0.047844**	**0.067922**
k4_ON_t_p	0.017255	0.019947	0.053326	0.042767	0.054525
k4_ON_t_r	0.026816	0.023325	0.055215	0.055294	0.038509
k4_ON_t_ts	0.026675	0.019207	0.054295	0.045935	0.048625
l4_ON_s_r	**0.033058**	**0.029294**	**0.070215**	**0.070859**	**0.043750**
l4_ON_t_p	0.017807	0.026133	0.057391	0.064056	0.046300
l4_ON_t_r	0.008513	0.018785	0.022822	0.001313	0.454029
l4_ON_t_ts	0.018637	0.024699	0.057885	0.060600	0.048031

Table 7: PDI Values (in e) for the different rings in NO molecule for reactants, transition state and products.

	PDI1	PDI2	PDI3	PDI4	PDI5
b_NO_s_p	**0.037943**	**0.059234**			
b_NO_s_r	**0.024160**	**0.082500**			
b_NO_s_ts	**0.036784**	**0.069818**			
b_NO_t_r	0.017552	0.040918			
k_NO_s_p	**0.037573**	**0.034246**	**0.082501**		
k_NO_s_r	**0.029628**	**0.055283**	**0.077149**		
k_NO_s_ts	**0.038533**	**0.045418**	**0.079307**		
k_NO_t_p	0.013701	0.034172	0.061962		
k_NO_t_r	0.013487	0.025738	0.070575		
k_NO_t_ts	0.016124	0.026976	0.067867		
l_NO_s_p	**0.033541**	**0.055582**	**0.059563**		
l_NO_s_r	**0.017610**	**0.062110**	**0.070600**		
l_NO_s_ts	**0.031661**	**0.057609**	**0.062886**		
l_NO_t_p	0.014694	0.020957	0.065112		
k4_NO_s_p	**0.035400**	**0.038684**	**0.032591**	**0.054910**	**0.067167**
k4_NO_s_r	**0.023922**	**0.053416**	**0.040206**	**0.046960**	**0.068136**
k4_NO_s_ts	**0.034351**	**0.045351**	**0.036176**	**0.050902**	**0.067645**
k4_NO_t_p	0.021117	0.018153	0.055328	0.044251	0.050064
k4_NO_t_r	0.024348	0.024462	0.054973	0.057861	0.038031
k4_NO_t_ts	0.032512	0.021292	0.055509	0.054088	0.040212
l4_NO_s_p	**0.038100**	**0.019597**	**0.072618**	**0.477778**	**0.044745**
l4_NO_s_r	**0.033700**	**0.031281**	**0.070221**	**0.466968**	**0.043769**
l4_NO_s_ts	**0.040670**	**0.026570**	**0.070987**	**0.470978**	**0.044120**
l4_NO_t_p	0.016312	0.024084	0.053593	0.471103	0.048313
l4_NO_t_r	0.013007	0.033559	0.045158	0.415858	0.059469
l4_NO_t_ts	0.016487	0.024396	0.055282	0.440557	0.054412